FR8600233

LP_201.

RP 137 (29)

UNIVERSITÉ DE PARIS-SUD - CENTRE D'ORSAY

LABORATOIRE DE

PHYSIQUE DES GAZ ET DES PLASMAS

(Laboratoire associé au CNRS)

27

Bâtiment 212 - 91405 ORSAY CEDEX (France) - Tél. 941-72-51

RP 137 (20)

ELECTRON ENERGY DISTRIBUTIONS AND EXCITATION RATES IN HIGH-FREQUENCY ARGON DISCHARGES.

C.M. FERREIRA and J. LOUREIRO

Rapport L.P. 201
Juin 1983.

Submitted to J. Phys. D : Appl. Phys.
19 May 1983

ELECTRON ENERGY DISTRIBUTIONS AND EXCITATION RATES IN HIGH-FREQUENCY ARGON DISCHARGES.

C. M. Ferreira[a), b)] and J. Loureiro[b)]

a) Laboratoire de Physique des Gaz et des Plasmas†, Université de Paris-Sud, 91405 Orsay Cedex, France.

b) Centro de Electrodinâmica da Universidade Técnica de Lisboa(INIC), Instituto Superior Técnico, 1096 Lisboa Codex, Portugal.

ABSTRACT - The electron energy distribution functions and rate coefficients for excitation and ionisation in argon under the action of an uniform high-frequency electric field were calculated by numerically solving the homogeneous Boltzmann equation. The treatment is restricted to situations in which the electrons do not lose appreciable energy during a cycle of field oscillation. Analytic calculations in the limiting cases $\omega \gg \nu_c$ and $\omega \ll \nu_c$, where ω is the wave angular frequency and ν_c is the electron-neutral collision frequency for momentum transfer, are also presented and shown to be in very good agreement with the numerical computations. The results reported here are relevant for the modelling of high-frequency discharges in argon and, in particular, for improving recent theoretical descriptions of a plasma column sustained by surface microwaves.

† - Laboratory associated with the Centre National de la Recherche Scientifique.

1 - INTRODUCTION

High-frequency gas discharges have long been the subject of intensive theoretical and experimental studies. In the last few years the possibility of creating and sustaining long, quiescent and reproducible plasma columns by the propagation of surface microwaves brought about a renewed interest in this field of research. In fact, the properties of surface wave produced plasmas make them interesting as possible substitutes for other more conventional plasma sources for such important applications as plasma chemistry, laser excitation, plasma etching, spectroscopic sources, etc. (for a review of the properties and applications of surface wave produced plasma see, e.g., Moisan et al 1982).

One problem of fundamental importance in the theoretical treatment of high-frequency gas discharges is the determination of the electron energy distribution function, excitation and ionisation rates, and transport parameters as a function of the amplitude and frequency of the HF electric field, and the gas pressure. Work through the 1940's and 1950's provided methods for calculating the electron energy distribution from the Boltzmann equation (see, e.g., Holstein 1946, Brown 1956, Allis 1956) but, by that time, solutions obtained using simplified cross section models were only investigated.

The present paper is concerned with the calculation of electron energy distributions and inelastic rate coefficients in argon under the influence of a high-frequency a.c. field by numerically solving the Boltzmann equation, using presently available cross section data. The treatment is restricted, in particular, to cases in which the frequency is sufficiently high so that the electrons do not lose appreciable energy during a cycle of field oscillation. Apart from this restriction, the calculations cover the whole range from $\omega \ll \nu_c$ to $\omega \gg \nu_c$, where ω is the angular frequency

of the HF field and ν_c is the electron-neutral collision frequency for momentum transfer. For $\omega << \nu_c$ the distribution function associated with an a.c. field of amplitude Ep is identical with that associated with a d.c. field $E = Ep/\sqrt{2}$ (Holstein 1946) and depends only on E/N, where N is the neutral gas density. The results obtained in this limit are shown to go over to those obtained previously for the d.c. case by Ferreira and Ricard (1983) and Ferreira and Loureiro (1983). For $\omega >> \nu_c$ the energy distribution is a function only of Ep/ω. Analytic calculations of the electron energy distributions in these two limiting situations are also presented and shown to agree remarkably well with the numerical computations.

The results reported here are relevant for the modelling of high-frequency argon discharges and, in particular, for improving recent models of low-pressure argon plasma columns sustained by surface microwaves (Ferreira 1981, 1983).

2 - FUNDAMENTAL EQUATION FOR THE ELECTRON ENERGY DISTRIBUTION

The situation to be considered here is that of a stationary gas discharge sustained by an uniform high-frequency field $E = E_p \exp(j\omega t)$. We assume that: (a) the field amplitude and the diffusion gradients are sufficiently small so that the distribution function can be well represented by a two-term expansion in spherical harmonics. This requires, in particular, that the diffusion cross section be much larger than the total inelastic cross section and that the electron mean free path be much less than any dimension of the discharge vessel (Holstein 1946, Brown 1956); (b) the frequency is sufficiently high so that the isotropic part of the distribution does not change appreciably during a cycle of field oscillation. This assumption is valid provided $\omega >> \tau_c^{-1}$ and $\omega >>$ v/smallest dimension of the

discharge vessel, where τ_e is the characteristic time for energy relaxation by collisions with the atoms and v is the electron velocity (note that the characteristic times for energy relaxation by elastic and inelastic collisions are $(m\nu_c/M)^{-1}$ and ν_x^{-1}, respectively, where ν_x is the total inelastic collision frequency, m is the mass of the electron and M is that of the atom); (c) the electron fluxes in configuration and velocity spaces resulting from the diffusion gradients and the space-charge field are small and both can be neglected, i.e., the electron energy distribution is essentially determined by the external a.c. field and the energy losses associated with elastic and inelastic collisions (for a discussion of space-charge field effects on the electron distribution function see, e.g., Bernstein and Holstein 1954 and Blank 1960).

Under the assumptions above and following standard procedures (see, e.g., Holstein 1946) the fundamental equation obtained for the isotropic part of the electron distribution function, f, is

$$-\frac{\partial}{\partial u}\left[u^{3/2}\,\nu_c\,\left(u_c\,\frac{df}{du}+\frac{3m}{M}f\right)\right]=\nu_x(u)f(u)\sqrt{u}-$$

$$-\sum_K \nu_K(u+v_K)f(u+v_K)\sqrt{u+v_K}. \qquad (1)$$

Herein,

$$u_c=\frac{e}{m}\,\frac{1}{\nu_c^2+\omega^2}\,\frac{E_p^2}{2} \qquad (2)$$

is the average energy transferred from the field to the electrons per collision (thus, $\nu_c u_c$ is the power transfer), $u = mv^2/2e$ is the electron energy in electron volts, e is the electron charge, ν_K is the collision frequency for an electron-induced transition from the ground state to the Kth level, v_K is the threshold energy for this process, and $\nu_x = \sum_K \nu_K$ is the total inelastic collision frequency. The normalisation for the distribution is $\int_0^\infty f\sqrt{u}\,du = 1$.

Eq. (1) expresses the continuity of the electron flux in energy space. The two terms in the brackets in the left-hand member represent the fluxes in energy space driven by the field and recoil (heating of the electron gas upon collisions with neutrals was neglected), respectively, while on the right are the terms representing the removal of electrons from a given energy range by inelastic collisions and their reappearance at lower energies. The energy loss associated with the ionisation process was assumed constant and equal to the ionisation threshold (thus the sum over K includes the ionisation process also). This is equivalent to assuming that the secondary electrons appear with zero energy but the effects of secondary electron production, at a rate which just compensates for the ambipolar diffusion loss, were neglected here. (Note, however, that this source term as well as the diffusion and space-charge field terms also neglected in Eq. (1) are essential for describing the discharge maintenance conditions. Indeed, only these terms contribute to the electron continuity equation as the integrals from zero to infinity of the two members of Eq. (1) both vanish).

Inspection of Eq. (1) reveals that the dependence of the distribution on the independent parameters E_p, ω, and N arises only through the average energy gain per collision u_c defined by Eq.(2). When $\nu_c >> \omega$ throughout the significant electron energy range we have $u_c = e E_p^2/2m\nu_c^2$ which is the same as the average energy gain per collision in a d.c. field $E = E_p/\sqrt{2}$, and the distribution is a function only of E/N. At the opposite limit, i.e., for $\omega >> \nu_c$, we have $u_c = e E_p^2/2m\omega^2$ and the distribution is a function only of E/ω. It becomes a function of any two parameters chosen from the set E/N, E/ω, ω/N in between. In the following, however, we will find it preferable replacing ω/N by the dimensionless variable ω/ν_{CM}, where $\nu_{CM} = N(\sigma_c\, v)_{MAX}$ is the maximum of ν_c in the energy range of interest here (see below for further details).

Eq. (1) was solved numerically using a self-consistent set of inelastic cross sections derived recently for argon by these authors (Ferreira and Loureiro 1983). We recall that this set has been obtained by numerically solving the homogeneous Boltzmann equation for the case of a d.c. field and making adjustments in the experimental cross section data available from the literature so that Boltzmann-derived and measured electron transport quantities be in agreement. The results of the present calculations will be given in Section 4. Firstly, however, some physical insight may be obtained by carrying on the calculations analytically for a number of specific cases, using appropriate cross section models.

3 - ANALYTIC CALCULATIONS

3.1 - General expressions

Above the lowest excitation threshold, V_x, the distribution decreases steeply so that the reintroduction of electrons may be neglected in this range. Therefore, the equation for the tail ($u > V_x$) becomes

$$\frac{2}{3}\frac{d}{du}\left[u^{3/2}\nu_c\left(u_c\frac{df}{du}+\frac{2m}{M}f\right)\right] = \nu_x(u)f(u)\sqrt{u}\ . \qquad (3)$$

In the body ($u < V_x$) the excitation and ionisation frequencies are zero and integrating Eq. (1) from zero to u in this range yields

$$\frac{2}{3}u^{3/2}\nu_c\left(u_c\frac{df}{du}+\frac{2m}{M}f\right) = -\sum_K \int_{V_K}^{V_K+u}\nu_K(u)f(u)\sqrt{u}\ du \qquad (4)$$

In general, the functions $\nu_K f\sqrt{u}$ have a sharp maximum just above the excitation potential, i.e., most excitation processes take place in a narrow energy range just above the corresponding thresholds. Consequently, the scattered electrons have very little energy and each of the integrals in the right-hand member of Eq. (4) may be replaced, without much error, by its asymptotic value for $u \to \infty$. Noting that the average inelastic frequency

per electron for the process K is given by

$$\bar{\nu}_K = \int_{V_K}^{\infty} \nu_K(u) f(u) \sqrt{u}\, du, \qquad (5)$$

Eq. (4) may be approximately written

$$\frac{2}{3} u^{3/2} \nu_c \left(u_c \frac{df}{du} + \frac{3}{H} f\right) = -\bar{\nu}_x, \qquad (6)$$

where $\bar{\nu}_x = \sum_K \bar{\nu}_K$. This equation has the formal solution

$$f = f(V_x)\, e^{-W} \left[1 + \frac{1}{2} \frac{\bar{\nu}_x}{f(V_x)} \int_u^{V_x} \frac{e^W du}{u^{3/2} \nu_c u_c}\right], \qquad (7)$$

where

$$W = \int_{V_x}^{u} \frac{3n}{H} \frac{du}{u_c}, \qquad (8)$$

and $f(V_x)$ is the value of f at $u = V_x$, where the solutions for the tail and the body must be joined.

The distribution (7) has several interesting limiting forms according to the range of the various parameters involved. At low fields (higher pressures) the second term in the brackets, which accounts for the reappearance of electrons in the body, is negligible, and f reduces to a Druyvesteyn distribution (Druyvesteyn and Penning 1940)

$$f = f(V_x)\, e^{-W}. \qquad (9)$$

When $\omega \gg \nu_c$, the average energy gain per collision is independent of the electron energy ($u_c = e^2 E_p^2 / 2m\omega^2$) and Eq. (9) further reduces to a Maxwellian distribution with temperature

$$T_e = \frac{M}{3m} u_c = \frac{e M}{6 m^2} \left(\frac{E_p}{\omega}\right)^2. \qquad (10)$$

When the condition $\omega >> \nu_c$ is not satisfied the distribution (9) may deviate considerably from a Maxwellian and its exact shape depends on the particular variation law of ν_c with the electron energy (see below).

At high fields, or when recoil losses are negligible the distribution (7) reduces approximately to the form

$$f = f(V_x) \left[1 + \frac{\bar{\nu}_x}{2} \frac{}{f(V_x)} \int_u^{V_x} \frac{du}{u^{3/2} \nu_c u_c}\right] . \qquad (11)$$

The results summarized above were obtained since the 1940's (for a review see, e.g., Allis 1956) and to proceed further we now need appropriate cross section models for argon. We will use the following models proposed by Ferreira and Ricard (1983) for the momentum transfer cross section σ_c and the total inelastic cross section σ_x:

$$\sigma_c = \begin{cases} a_c \frac{u}{V_x} & \text{for } u \leq V_x \\ a_c \left(\frac{u}{V_x}\right)^{-1/2} & \text{for } u \geq V_x \end{cases} \qquad (12)$$

$$\sigma_x = a \left(\frac{u}{V_x}\right)^{-1/2} \left(\frac{u}{V_x} - 1\right) \text{ for } u \geq V_x \qquad (13)$$

with $a_c = 1.59 \times 10^{-15}$ cm^2 and $a = 1.56 \times 10^{-16}$ cm^2. These values were chosen so that calculated and measured electron transport parameters be in good agreement (for details, see Ferreira and Ricard 1983). Note that, according to (12), we have $\nu_c = \nu_{CM} (u/V_x)^{3/2}$ for $u \leq V_x$, and $\nu_c = \nu_{CM}$ for $u \geq V_x$, where $\nu_{CM}/N = 3.2 \times 10^{-7}$ cm^3 sec^{-1}.

Using these models analytic solutions can be readily derived as shown below.

3.2 - Solutions for the tail

In the tail ν_c is a constant, ν_{CM}, and introducing an effective field

$$E_f = \frac{E_p}{\sqrt{2}} \frac{\nu_{CM}}{(\nu_{CM}^2 + \omega^2)^{1/2}} , \qquad (14)$$

The solutions in this range are identical with those found previously for the case of a d.c. field of amplitude E_p (Ferreira and Ricard 1983). These solutions can be expressed in the terms of the confluent hypergeometric function U (Abramowitz and Stegun 1965) as

$$f = f(V_x)\left(\frac{u}{V_x}\right)^{-1/2} \exp\left[-(p_x+p_o)(u-V_x)\right] \frac{U(-\gamma, 1/2, (p_o+2p_x)u)}{U(-\gamma, 1/2, (p_o+2p_x)V_x)} , \qquad (15)$$

where

$$p_x = \frac{1}{2}\left[(p_o^2 + 4 q_o \alpha)^{1/2} - p_o\right] , \qquad (16)$$

$$p_o = \frac{m^2}{eM}\left(\frac{\nu_{CM}}{E_f}\right)^2 = \frac{m^2}{eM} \frac{\nu_{CM}^2 + \omega^2}{E_p^2} , \qquad (17)$$

$$q_o = 3\left(\frac{m}{2eV_x}\right)^{1/2} \frac{\nu_{CM}}{N}\left(\frac{m}{E_f}\right)^2 = 3\alpha_c\left(\frac{m}{E_f}\right)^2 \qquad (18)$$

$$\gamma = \frac{q_o \alpha V_x + \frac{3}{4} p_o}{p_o + 2p_x} - \frac{1}{4} . \qquad (19)$$

The average inelastic frequency per electron, $\bar{\nu}_x$, cannot be calculated analytically using Eq. (15), but it turns out that the exact solutions for the tail may reasonably well fitted by a function of the type $f = f(V_x)(u/V_x)^{\beta}\exp\left[-p_x(u-V_x)\right]$, provided the parameter β is appropriately chosen for each value of E_f/N. Using this approximation the calculation of $\bar{\nu}_x$ is straightforward and yields (see Ferreira and Ricard 1983)

$$\bar{\nu}_x = \left(\frac{2e}{m}\right)^{1/2} N f(V_x) \alpha V_x^2 U(2, \beta + \frac{7}{2}, p_x V_x) \qquad (20)$$

3.3 – Solutions for the body

When $\omega << \nu_c$, Eq. (7) reduces, after some manipulation, to the simpler form

$$f = f(V_x)\left[e^{P(1-x^4)} + \frac{2M}{m}\frac{\alpha}{\alpha_c} PU(2, \beta + \frac{7}{2}, p_x V_x) e^{-Px^4} \int_x^1 e^{Px^4} dx\right], \qquad (21)$$

where $x = u/V_x$, and we have introduced the dimensionless parameter

$$P = \frac{3m}{M}(\alpha_c V_x)^2 \left(\frac{N}{\Sigma_p}\right)^2 \qquad (22)$$

For $\Sigma_p/N >> (3m/M)^{1/2} \alpha_c V_x$, i.e., Σ_p/N somewhat larger than 10^{-16} V cm^2, we have $P << 1$ and the recoil losses are negligible. In this case, the solution for the body is quite simple, viz.,

$$f = f(V_x)\left[1 + \frac{2M}{m}\frac{\alpha}{\alpha_c} PU(2, \beta + \frac{7}{2}, p_x V_x)(1 - \frac{u}{V_x})\right] . \qquad (23)$$

At the opposite limit, i.e., at sufficiently, low fields such that the reappearance of electrons in the body is negligible (mathematically, this limit corresponds to $U(2, \beta + \frac{7}{2}, p_x V_x) \to 0$), the distribution reduces to the form

$$f = f(V_x)\, e^{P(1-x^4)} . \qquad (24)$$

When $\omega >> \nu_c$, we obtain from Eq. (7)

$$f = f(V_x)\left[e^{-(y-V)} + \frac{M}{3m}\frac{\alpha}{\alpha_c} V^3 U(2, \beta + \frac{7}{2}, p_x V_x) e^{-V} \int_y^V y^{-3} e^{y} dy\right], \qquad (25)$$

where we have defined $y = u/T_e$, $V = V_x/T_e$, and T_e is given by Eq. (10). The integral term in Eq. (25) can be expressed in terms of the exponential integral

function Ei(y) (Abramowitz and Stegun 1965) and we obtain after some manipulation

$$e^{-y}\int_y^V y^{-3}e^y dy = \frac{1}{y^2}\left[1+y(1-e^{-y}y\ \mathrm{Ei}(y))\right] - \frac{1}{V^2}\left[1+V(1-e^{-V}V\ \mathrm{Ei}(V))\right] \quad (26)$$

This term diverges as $u \to 0$ but this spurious infinity at the origin is due to our assumption that all scattered electrons reappear in the body with zero energy. The divergence would be eliminated if the exact behaviour of the second-hand member of Eq. (4) as $u \to 0$ were taken into account. Owing to the approximation used Eq. (25) deviates considerably from the true solution in the close vicinity of the origin (see Fig. 2, below).

At sufficiently low fields Eq. (25) reduces to a Maxwellian distribution $f = f(V_x)\ \exp\left[-(u-V_x)/T_e\right]$, as we have already pointed out. At high fields, we have $V_x/T_e \ll 1$ (T_e has no particular physical meaning in this case) and Eq. (25) reduces to the simpler form

$$f = f(V_x)\left[1+\frac{11}{4m}\frac{1}{\alpha_c}V^3 U(2,\beta+\frac{7}{2},\ p_x V_x)\left(\frac{1}{y^2}+\frac{2}{y}-\frac{1}{V^2}-\frac{2}{y}-\mathrm{Ln}\frac{y}{V}\right)\right], \quad (27)$$

which, for sufficiently small V, can be further reduced to the asymptotic form

$$f = f(V_x)\{1+Q\left[\left(\frac{V_x}{u}\right)^2-1\right]\}, \quad (28)$$

where

$$Q = \frac{11}{4m}\frac{\alpha}{\alpha_c}\frac{V_x}{T_e}U(2,\beta+\frac{7}{2},\ p_x V_x) = \frac{3}{4}\frac{\alpha}{\alpha_c}\frac{V_x}{u_c}U(2,\beta+\frac{7}{2},\ p_x V_x). \quad (29)$$

4 - RESULTS AND DISCUSSION

For the presentation and discussion of results it is interesting to refer to the $E/N - E/\omega$ diagram illustrated in Fig. 1, where $E = E_o/\sqrt{2}$ denotes the root-mean-square field. The line $R \equiv \omega/\nu_{CM} = 1$ shown on this diagram separates the two regions in which $\omega > \nu_{CM}$ and $\omega < \nu_{CM}$, respectively. In the upper($R > 1$) and lower ($R < 1$) half-planes the distribution becomes a function only of E/ω or E/N, respectively, excepting in a transition region in between where it depends on both parameters. The vertical line marked on the diagram corresponds to the value of E/ω ($\simeq 3 \times 10^{-10}$ V cm^{-1} sec) for which, in the case $\omega >> \nu_{CM}$, the energy losses by elastic and inelastic collisions are identical (see also Fig. 3 below). To the left of this vertical line (i.e., lower E/ω values) the body of the distribution Maxwellizes with T_e given by Eq. (10), while to the right (i.e., higher E/ω values) one enters into the domain of applicability of the approximations (27) and (28). A scale for the electron temperature is also provided in Fig. 1 which illustrates the relationship between E/ω and T_e values.

In practice, the body of the distribution may be a function only of E/ω, thus independent of N, provided ω is larger than some energy-averaged value of the collision frequency for momentum transfer (therefore, the condition $\omega >> \nu_{CM}$ appears to be too severe). A somewhat more appropriate condition could be, for instance, $\omega >> \bar{\nu}_c$, where

$$\bar{\nu}_c = -\frac{2}{3} \int_0^\infty \nu_c \, u^{3/2} \frac{df}{du} \, du \qquad (30)$$

(It is interesting to note that the condition $\omega >> \bar{\nu}_c$ is usually employed to characterize the low-attenuation regime for surface waves propagating along a plasma column. See, e.g., Ferreira 1981, 1983). For the purposes of illustration the line $R' = \omega/\bar{\nu}_c = 10$ is also marked on the $E/N - E/\omega$

diagram of Fig. 1. Here, $\bar{\nu}_c$ was calculated numerically, but an explicit analytic calculation can also be performed when the distribution is Maxwellian, using Eq. (12) for the momentum transfer cross section. We obtain in this case $\bar{\nu}_c = (8/\sqrt{\pi})(T_c/V_x)^{3/2}\nu_{CM}$, hence the equation for the lines R' = constant in the Maxwellian region is simply

$$\frac{E}{N} = \left(\frac{E}{\omega}\right)^4 R' \frac{2}{\sqrt{\pi}} \left(\frac{e\,M}{3\,m^2 V_x}\right)^{3/2} \frac{\nu_{CM}}{N} \quad . \tag{31}$$

As shown in Fig. 1, the numerical solution for the line R' = 10 goes over, in the Maxwellian region, exactly to the limit predicted by Eq. (31) (dot-dashed line).

Figure 2 shows calculated electron energy distributions in the limiting cases $\omega \ll \nu_{CM}$ and $\omega \gg \nu_{CM}$, for various values of E/N and E/ω, respectively. The dot-dashed lines represent analytic calculations based on the expressions derived in Sect. 3; they agree remarkably well with the numerical solutions, except at low electron energies in the case of curves A and B (the reasons for these discrepancies close to the origin have already been explained). Here, the numerical solutions are all normalised to one electron; the analytic solutions are normalised to the numerical ones at $u = V_x$ in the case of curves A and B ($\omega \gg \nu_{CM}$) and to one electron in the case of curves C and F, as the normalisation in the latter two cases could be performed analytically. As expected, for $E/\omega = 10^{-10}$ v cm^{-1} sec (curve C) the body of the distribution is a Maxwellian with $T_c = 0.43$ eV which agrees with the value predicted by Eq. (10).

Figures 3 (a) and 3 (b) show calculated distributions for various combinations of the parameters. The full curves in Fig. (3a) are for constant $\omega/N = 4 \times 10^{-7}$ cm^3 sec^{-1} (thus, $\omega/\nu_{CM} = 1.25$ which corresponds to a transition region on the diagram of Fig. 1) are various values of E/N. These distributions are considerably different in shape from those

obtained for a d.c. field and the same E/N values which are also shown for comparison. The distributions shown in Fig. 3(b) are for constant $E/N = 6.5 \times 10^{-16}$ V cm^2 and various values of $R \equiv \omega/\nu_{CM}$ ranging from zero (d.c. case) to 31.2 ($\omega/N = 0 - 10^{-5}$ cm^3 sec^{-1}). As R increases at constant E/N the representative point on the diagram of Fig. 1 moves along a horizontal straight line from the right to the left and penetrates into the Maxwellian domain at sufficiently high R. From Fig. 3(b) it is seen that the Maxwellization is practically achieved in this case for R > 15.

Hereafter, we shall be concerned with various energy averaged quantities, calculated in the limiting case $\omega >> \nu_{CM}$, which are relevant for the modelling of plasma columns sustained by weakly damped surface microwaves. For $\omega << \nu_{CM}$ the results are identical with those reported elsewhere for a d.c. field (Ferreira and Ricard 1983, Ferreira and Loureiro 1983) and need not be further discussed here.

The electron power balance equation is obtained by multiplying both members of Eq. (1) by the electron energy and, then, integrating over the whole energy range. This yields, for $\omega >> \nu_{CM}$,

$$\frac{1}{2}\frac{e}{m}\bar{\nu}_c\left(\frac{E_p}{\omega}\right)^2 = \frac{2m}{M}\langle u\,\nu_c\rangle + \sum_K \bar{\nu}_K\,\nu_K\,, \qquad (32)$$

where $\bar{\nu}_c$ and $\bar{\nu}_K$ are defined by Eqs. (30) and (5). The term in the left-hand member represents the average power input from the field, while the first and second terms on the right represent the elastic and inelastic power losses, respectively (the symbol $\langle\ \rangle$ denotes an energy-averaged value). When the elastic losses are dominant the distribution is a Maxwellian and, in this case, $(2\,m/M)\langle u\,\nu_c\rangle = (3m/M)T_e\,\bar{\nu}_c$. Equating this to the average power input from the field and solving for T_e yields Eq. (10).

The fractional electron energy losses by elastic and inelastic collisions are presented in Fig. 4 as a function of E/ω. Under typical

operating conditions the values of E/ω required for sustaining a low-pressure plasma column by surface microwaves lie in the range from about 5×10^{-10} to 10^{-8} V cm^{-1} sec, depending on the pressure-radius product pa (for pa $\leq$ 1 Torr cm and wave frequencies from 360 to 2450 MHz; see, e.g., Ferreira 1981, 1983). Therefore, the inelastic losses are predominant in this type of plasma.

Figures 5 shows the variation of $\bar{\nu}_c/N$ and $\sum_K V_K \bar{\nu}_K/N$ with E/ω. When the distribution is Maxwellian we have already obtained analytically $\bar{\nu}_c = (3/\sqrt{\pi})(T_e/V_x)^{3/2} \nu_{CM}$, which combined with Eq. (10) yields

$$\frac{\bar{\nu}_c}{N} = \frac{8}{\sqrt{\pi}} \left(\frac{eM}{3m^2 V_x}\right)^{3/2} \frac{\nu_{CM}}{N} \left(\frac{E}{\omega}\right)^3 \quad . \tag{33}$$

As seen from Fig. 5 the curve of $\bar{\nu}_c/N$ has, indeed, the asymptotic behaviour predicted by Eq. (33) (dot-dashed line shown on the figure) at low E/ω. At higher E/ω, when the inelastic losses become predominant, the numerical solutions may be well fitted by the simple empirical laws $\bar{\nu}_c/N \propto (E/\omega)^{0.4}$ and $\sum_K V_K \bar{\nu}_K/N \propto (E/\omega)^{2.4}$.

Finally, the electron rate coefficients for direct excitation of the $^3P_2$ and $^3P_0$ metastables, $^3P_1$ and $^1P_1$ resonant levels, lumped forbidden levels (with a threshold of 12.9 eV) and lumped higher-lying allowed levels (with a weighted threshold of 14.25 eV), and the ionisation rate coefficient are shown in Fig. 6 as a function of E/ω.

For the purposes of rough estimates and interpretation of experiments the calculated excitation coefficients may be approximately fitted by a simple power law of the type $C_K \propto (E/\omega)^{a_k}$ for $5 \times 10^{-10} < E/\omega < 10^{-8}$ V cm^{-1} sec, with the following a_k values corresponding to the various excitation processes: 1.7 for the lumped $^3P_2$ and $^3P_0$ metastables; 2.0 for the $^3P_1$ and $^1P_1$ resonant levels; 2.9 for the groups of

forbidden and higher-lying allowed levels. A similar power law with $a_K = 4.1$ yields also a reasonable fit to the ionisation rate for $10^{-9} < E/\omega < 10^{-8}$ V cm^{-1} sec. Recent intensity measurements of the ArI 425.9 nm line emitted by the $3p_1$ level (Paschen notation), situated at 14.74 eV from the ground, in a surface wave produced plasma column ($f = 2.45$ GHz; pa = 0.03 - 0.75 Torr cm; E/ω = (0.6 - 10) $\times 10^{-9}$ V cm^{-1}sec) have shown that the intensity I_λ is proportional to $n_e N \bar{E}^3$, where n_e is the electron density and $\bar{E}$ is the radially averaged amplitude of the wave field (Laporte et al 1983). This experimental result can be well explained assuming predominant direct excitation and a variation of the rate coefficient as $(E/\omega)^3$, which agrees remarkably well with the present prediction of the variation of the excitation rates for the forbidden and higher-lying allowed levels.

In conclusion, the results reported here are useful for the modelling of high-frequency argon discharges and for the interpretation of current experiments being conducted with surface wave produced argon plasmas. In particular, the present results permit us to improve recent theoretical work concerned with the modelling of this type of plasmas in which a Maxwellian electron energy distribution was assumed (Ferreira 1981, 1983).

ACKNOWLEDGMENTS

One of us (CMF) would like to thank the Centre National de la Recherche Scientifique for the award of a visiting Fellowship during the early part of this work carried out at the Laboratoire de Physique des Gaz et des Plasmas, Universite de Paris-Sud, Orsay (France).

REFERENCES

Abramowitz M. and Stegun I.A. (eds.) 1965 Handbook of Mathematical Functions (Dover, New York).

Allis W.P. 1956 Handbuck der Physik 21, 383-444.

Bernstein I.B. and Holstein T. 1954 Phys. Rev. 94, 1475-82.

Blank J.L. 1966 Phys. Fluids 11, 1686 - 98.

Brown S.C. 1956 Handbuck der Physik 22, 531-75.

Druyvesteyn M.J. and Penning F.M. 1940 Rev. Mod. Phys. 12, 87.

Ferreira C.M. 1981 J. Phys. D: Appl. Phys. 14, 1811-30.

Ferreira C.M. 1983 J. Phys. D: Appl. Phys. (in press).

Ferreira C.M. and Ricard A. 1983 J. Appl. Phys. (April issue).

Ferreira C.M. and Loureiro J. 1983 J. Phys. D: Appl. Phys. (in press).

Holstein T. 1946 Phys. Rev. 70, 367 - 84.

Laporte C., Bloyet E., Dervisevic E., Leprince P., Marec J., Pouey M., and Sadda S. 1983 contributed paper to the XVI Int. Conf. Phenom. Ioniz. Gases (Düsseldorf, F.R. Germany).

Moisan M., Ferreira C.M., Hajlaoui Y., Henry D., Hubert J., Pantel R., Ricard A., and Zakrzewski Z. 1982 Rev. Phys. Appl. 17, 707-27.

Figure captions

Fig. 1 - E/N - E/ω diagram. Solid lines : A - R ≡ ω/ν_{CM} = 1; B - R' ≡ $\omega/\bar{\nu}_c$ = 10; C - E/ω = 3×10^{-10} V cm^{-1} sec (equality between the elastic and inelastic loss rates in the case R >> 1). The dot-dashed line is the theoretical asymptotic limit of the line R' = 10 at low E/ω.

Fig. 2 - Calculated electron energy distributions. Solid lines-numerical; dot-dashed lines-analytical. Curves A, B, and C are for $\omega >> \nu_{CM}$ and the following values of E/ω in 10^{-9} V cm^{-1} sec : A - 5.55; B - 1.38; C - 0.1. Curves D and F are for $\omega \ll \nu_{CM}$ and the following values of E/N in 10^{-16} V cm^2 : D - 8.88; F - 4.44.

Fig. 3 - Calculated electron energy distributions. (a) Solid curves: R ≡ ω/ν_{CM} = 1.25; dashed curves: R << 1 (d.c. case). The different curves are for the following values of E/N in 10^{-16} V cm^2: A - 10; B - 6.5; C - 3; D - 1.5. (b) For E/N = 6.5×10^{-16} V cm^2 and the following values of R ≡ ω/ν_{CM} : A - 0 (d.c. case); B - 1.25; C - 9.35; D - 15.6; F - 23.4; G - 31.2.

Fig. 4 - Fractional electron energy losses vs. E/ω in the case $\omega >> \nu_{CM}$: A - elastic losses; B - total inelastic losses.

Fig. 5 - Rate of inelastic losses per electron (curve A) and average collision frequency (curve B), at unit gas density, as a function of E/ω in the case $\omega >> \nu_{CM}$. The dot-dashed line is the theoretical asymptotic limit of curve B at low E/ω.

Fig. 6 - Electron rate coefficients for ionisation (curve G) and direct excitation of the following levels and groups of levels: A - $^3P_1$; B - $^1P_1$; C - $^3P_2$ + $^3P_0$; D - forbidden levels (threshold - 12.9 eV); F - higher-lying allowed levels (weighted threshold - 14.25 eV).

Fig.1

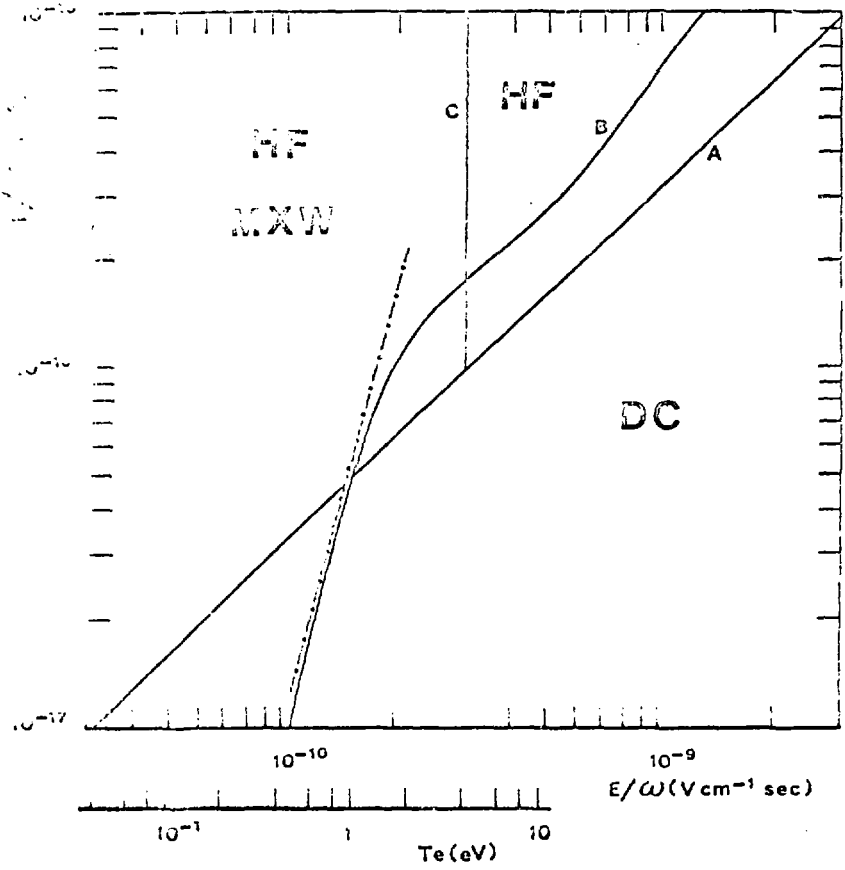

Fig.2

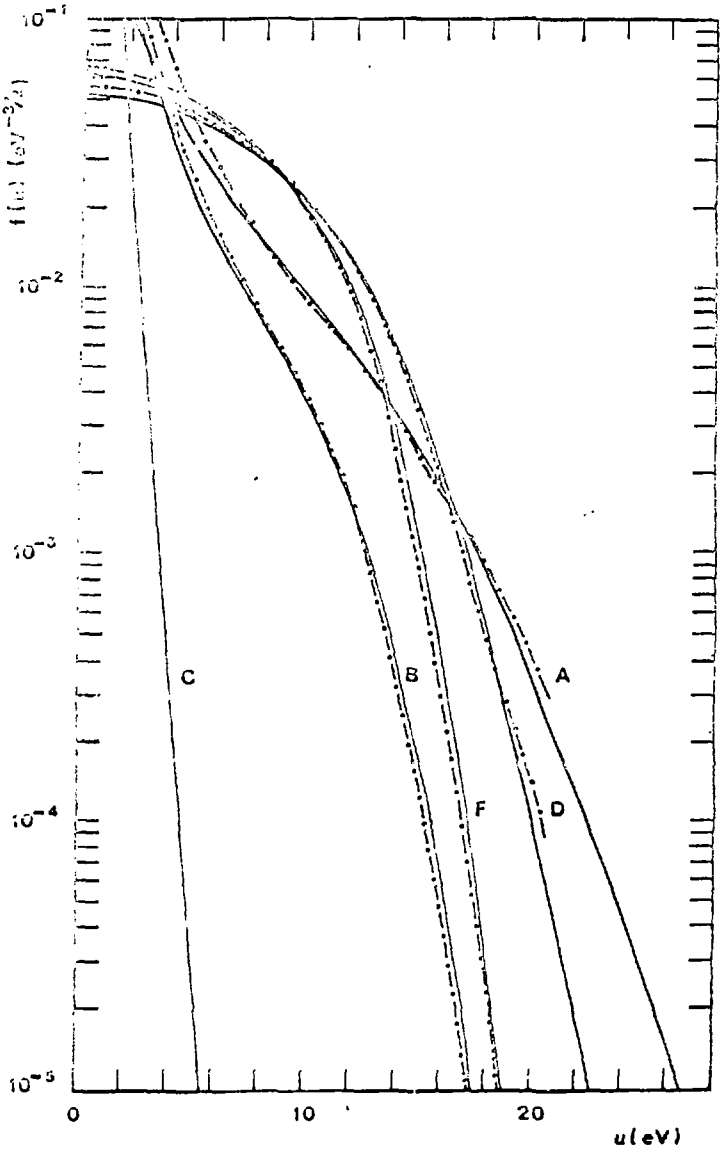

Fig. 3(a)

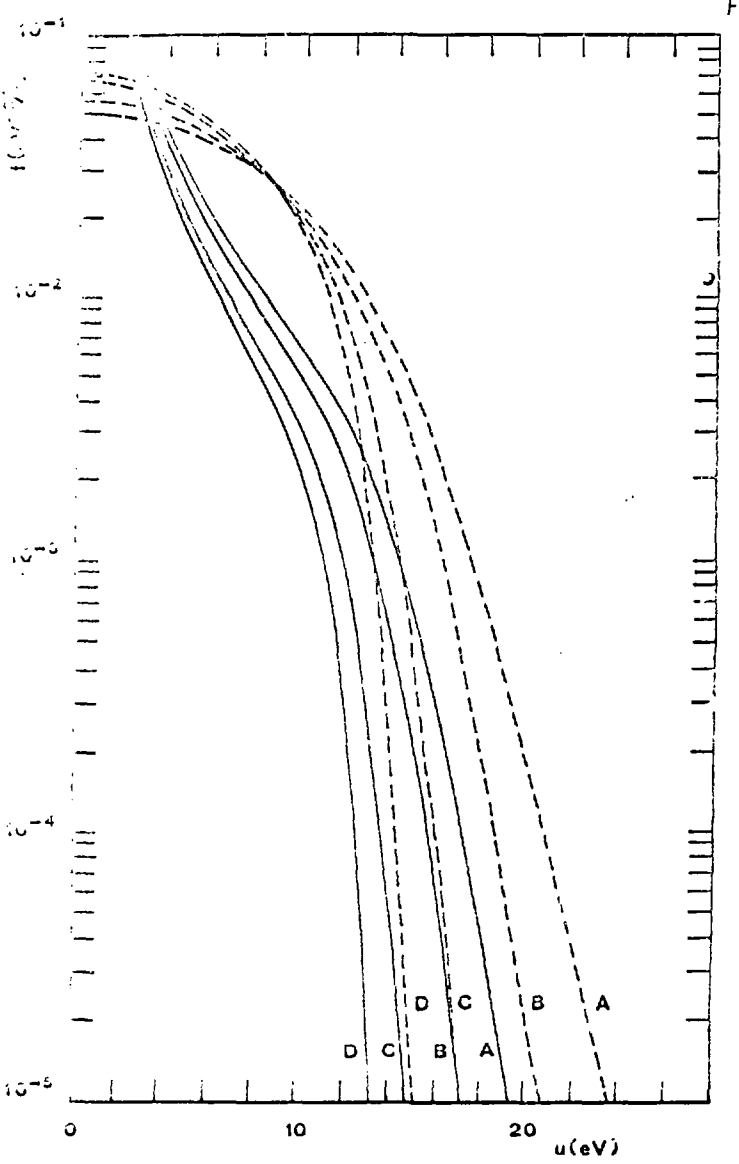

Fig. 3(b)

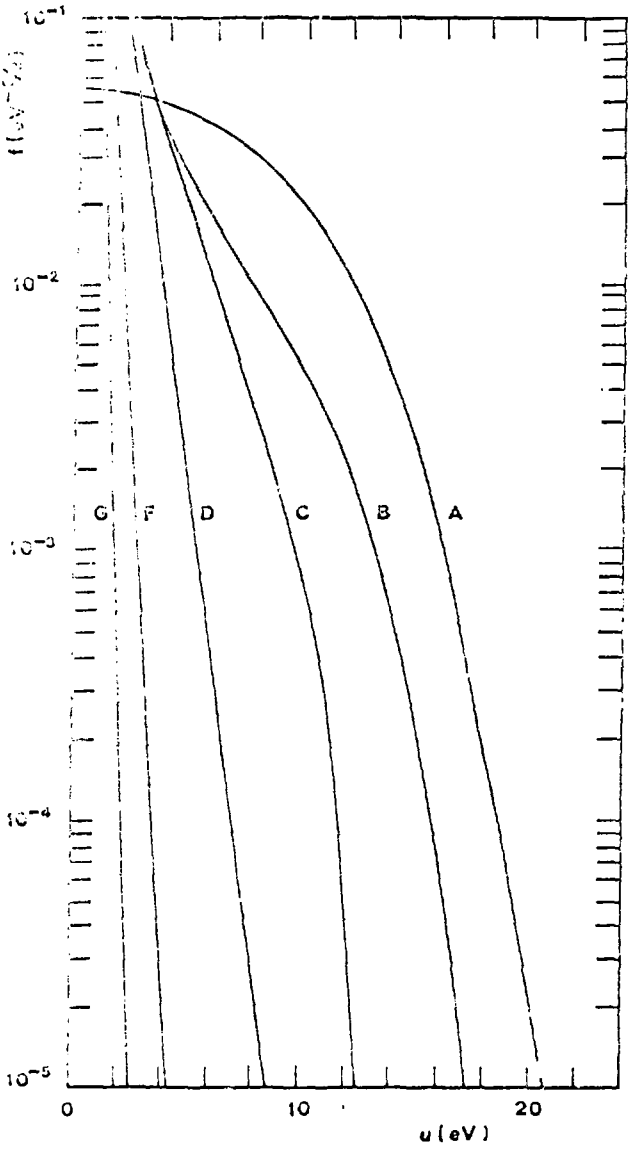

Fig. 4

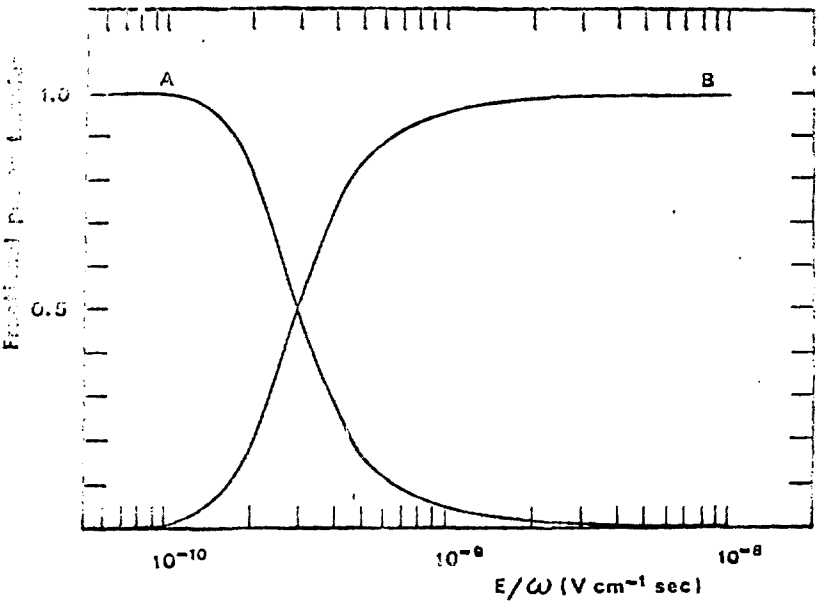

Fig.5

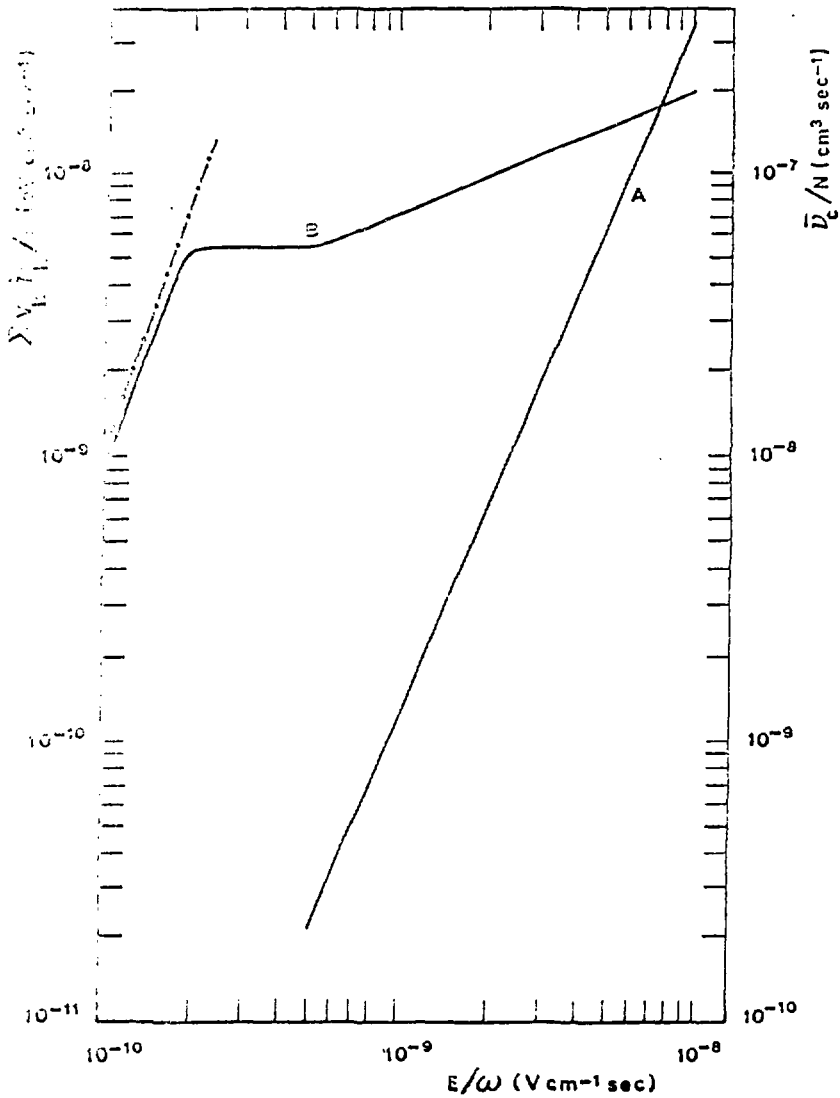
10^{-8}
10^{-9}
10^{-10}
10^{-11}
10^{-7}
10^{-8}
10^{-9}
10^{-10}
10^{-10}
10^{-9}
10^{-8}
B
A
$\bar{\nu}_e/N$ (cm^3 sec^{-1})
E/ω (V cm^{-1} sec)

Fig. 6

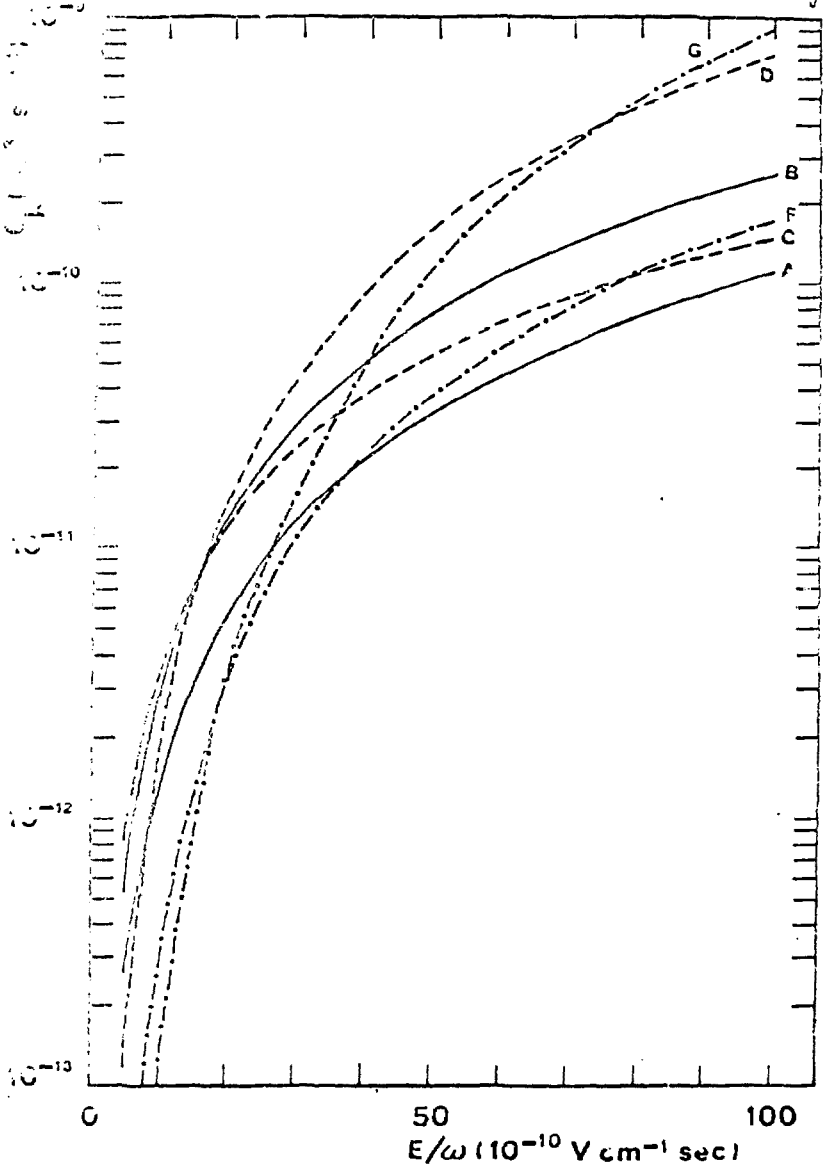

Réalisé avec le concours du service imprimerie de la 7ème Circonscription
1, Place Aristide-Briand – 92190 Meudon – Tél. 534 75 50 – Telex 204125